Journal of Operation and Automation in Power Engineering
Vol. 10, No. 2, Aug. 2022, Pages: 165-174
http://joape.uma.ac.ir

# Evaluation of Delays-based Stability of LFC Systems in the Presence of Electric Vehicles Aggregator

*F. Babaei**, *A. Safari, J. Salehi*

*Department of Electrical Engineering, Azarbaijan Shahid Madani University, Tabriz, Iran*

***Abstract***-*In the integrated electrical systems, frequency control service considering the electric vehicle (EV) aggregators could lead to time-varying delay in load frequency control (LFC) schemes. These delays influence the LFC system efficiency, and in some situations, the lack of a clear choice of a control strategy considering the time-varying delays causes power system instability. Thus, this paper illustrates different time-varying delays based on the stability of an LFC system in the EV aggregators presence. The LFC's delay-dependent stability study is executed for finding the stability region and, stability criteria is suggested using the linear matrix inequality (LMI) method and Lyapunov-Krasovskii theory. Also, Wirtinger-based improved inequality and bounding lemma are applied to compute the greatest allowable delay in the LFC system, including the EV aggregators.*

***Keyword:*** Electric vehicle Aggregator, LMI, Lyapunov-Krasovskii theory, Load frequency control, Stability analysis, Time-varying delay.

## 1. INTRODUCTION

### 1.1. Motivation

Nowadays, because of environmental problems and the gradual diminution of fossil resources, Electric vehicles (EVs) have been widely attended. Moreover, EVs have some main features, such as less noise pollution and high-efficiency. The EV participation in demand response and power generation leads to increase energy supply resilience. On the other hand, the vehicle-to-grid (V2G) technique allows for the return of stored energy in their idle time (park time) to the network during the peak demand period [1]. Using electric services with quick response for balancing the load fluctuations and improving power system performance has been known as the main advantages of V2Gs [2]. The EVs can provide frequency control service in order to improve the power systems operation. According to the wide application of EVs in the current power systems and their high potential for participating in the ancillary services markets like frequency control service, the structure of the conventional load frequency control (LFC) systems has been changed [3]. Besides, the open communication networks like the Internet, WiMax and WiFi that transfer the control signal to EVs could lead to time-varying delays. The time delays significantly affect the network frequency's stability, especially when the size of the time delay is close to or greater than the delay margin. Accordingly, it is worth noting that the LFC's delay-based stability considering the EV aggregators should be considered more.

### 1.2. Review of literature

Existing electricity markets allocate a multi-billion-dollar annual income to help the V2G development. Thus, V2Gs increase the reliability indices and reduce the power system operation cost. As described in Ref. [4], V2G plays a fundamental role in the 21st-century electric system based on renewable energy sources. Decentralized V2G technology was suggested for EVs participation in frequency control in Ref. [5]. Using EVs or other controllable loads for system frequency regulation was examined in the literature [6, 7]. The batteries of EVs could exchange power with the network faster than conventional generators. Therefore, the dynamic stability of the LFC system increases considering the EVs.

On the other hand, for more participation of the EVs owner in ancillary services, encouragement policies must be applied. The EV aggregators are the user interface between the residential customers and the independent system operator. It creates a mutually beneficial connection between EV owners and the electrical system. Consequently, the profits coming from

Received: 09 Jun. 2021
Revised: 01 Jul. 2021
Accepted: 05 Jul. 2021
∗Corresponding author:
E-mail: f.babaei@azaruniv.ac.ir (F. Babaei)
DOI: 10.22098/joape.2022.9042.1626
***Research Paper***

energy trading are maximized in the power market [8]. For the independent system operator, EV aggregators act as a large size of the generation or load which are controllably used in the ancillary services. The EV aggregators take part in the day-ahead and daily power market with production and consumption energy bids. It should be noted that the bidding strategy of the EV aggregator was formulated as a bi-level problem [9]. The effect of time-varying delays in EV aggregators in their frequency control and mileage payments was investigated in Ref. [10]. The power output of all generating units in power plants is determined by automatic generation control (AGC) system. In the AGC system, the control instructions are sent to EVs by communication networks. The communication network is classified into two categories: dedicated and open networks [11]. The access rate to communication resources through the obvious relation between cost and pricing is determined in the open communication network. These networks are used due to their low costs in an AGC system, but they cause a time-varying delay in an LFC system. As described, the EVs have a fast-response facing load oscillations, but these time-varying delays in EV aggregators could cause power system instability. The LFC system stability analysis is important because of delayed response effects on EV aggregators in the frequency control. Due to the development of the phasor measurement units and open communication networks in the modern electrical system, time-varying delays-based stability has been attracted. The time-delayed LFC systems stability includes the following issues: calculating the delay margin and designing the parameters of the controller. Delay margin is the greatest allowable delay to ensure the power system stability at the evaluated controller parameters. The delay-based robust control of a PID-type LFC system was proposed in Ref. [12]. In order to investigate the time delay effects on the stability of one and two-area LFC systems, an analytical method to assign the upper bound of the delay was introduced in Ref. [13]. The delay-dependent-matrix-based estimation method was introduced as one of the stability analysis techniques of the time-varying delay systems. The estimation approaches could achieve less conservative stability criteria in the form of the linear matrix inequality (LMI) [14]. The LMI based delay-dependent stability analysis methods have mainly been used in the delayed LFC system. But, the calculation burden of solving large-scale LMIs is known as a major challenge of the real-world power system. To improve the numerical tractability of delay-dependent stability, the chordal sparsity and symmetry of the graph related to LFC loops were presented in Ref. [15]. Criteria for the delay-dependent stability determination of multi-area LFC scheme including unknown and time-varying load oscillation is presented in Ref. [16]. The microgrid stability in the presence of plug-in EVs and communication delay was investigated by Khalil et al. [17]. At first, the microgrid model with time delay was presented and then Lyapunov-Krasovskii function as the desired stability criteria was employed. Finally, the upper bound of the delay was computed in such a way that the microgrid stability was ensured. The delay margin of the LFC schemes was investigated in the presence of constant time delay in Ref. [18]. To carry out the delay-dependent stability analysis in the multi-area LFC schemes that faced with the problem dimension increment, an improved LMI-based criterion was introduced in Ref. [19]. The interaction of delay margins and PID controller gain in the traditional and deregulated multi-area LFC system is well investigated. It should be noted that the proposed criterion is less conservative than the previous criteria. The fractional-order PI controller for a sample LFC system with time delay was proposed in Ref. [20]. A robust LFC for a one-area power network considering uncertain parameters and time delays in data transfer was designed and analyzed in Ref. [21]. The issue of delay-dependent stability for achieving the stability region that ensures the LFC scheme's desired efficiency is not investigated in the literature. In the case of multiple time-varying delays-dependent stability regions, few works of literature were performed in the control area. The augmented Lyapunov–Krasovskii function was used to obtain the new stability criteria with delay dependency in terms of LMIs in the LFC system. Intermediate auxiliary functions, which result in creating tighter bounds than Wirtinger double integral inequality was introduced for the stability analysis of LFC systems with interval time-varying delay in Ref. [22]. To reduce the calculation burden of delay-dependent stability analysis as well as improving computation accuracy in the large-scale multi-area LFC scheme, an augmented Lyapunov functional and Wirtinger inequality is proposed to maintain a stable condition with less conservatism [23]. The proposed stability criterion could lead to obtaining an accurate delay margin in the frequency domain. Delay-dependent stability analysis of LFC system containing EV aggregators with single and multiple time-varying delays was carried out in Ref. [24]. Also, the maximum allowable delay of EV aggregators for different PI controller parameters and participation ratio was presented. The main purpose of our paper is to reduce the conservatism of the greatest allowable delay calculation. According to the obtained results in Ref. [24], the value of the greatest allowable delay was increased. In this paper, the model presented in Ref. [24] was extended by including the LFC system's stability region and its root locus.

### 1.3. Contributions

The LFC's stability problem with participating in the EV aggregators in frequency control has a characteristic of time-varying delays. The major contributions of this study can be presented as:

- Evaluation of different time-varying delays based on the stability of the LFC system in the presence of the EV aggregators
- Modification of the LFC system model containing EV aggregators in terms of delay
- Calculation of the stability regions and criteria by using linear matrix inequality approach and Lyapunov-Krasovskii theory
- Exploring the participation ratio of the EV aggregators on the greatest allowable delay.

## 2. EV AGGREGATOR WITH TIME VARYING DELAYS BASED LFC SYSTEM

Electric vehicle aggregators are assumed to be able to provide the frequency control service by many available EVs. In this regard, the control center sends the commands to EV aggregators to eliminate the power oscillations. After the command reception, the contribution of each EV for participating in frequency control is determined. Transferring data through the communication network has a time delay. Thus, each EV will have a delayed response. For small-signal stability analysis, a linearized dynamic model of all components of the system is required. Different types of conventional LFC schemes were presented in several papers. A one-area LFC scheme by considering the numerous EV aggregators with time-varying delays is introduced in Fig. 1.

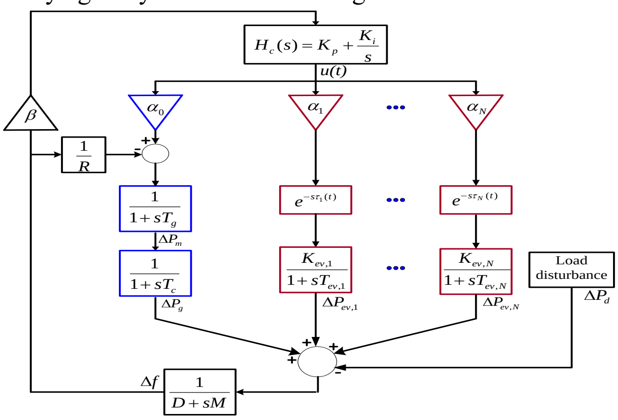


**Fig. 1. LFC system containing numerous EV aggregators considering time-varying delays**

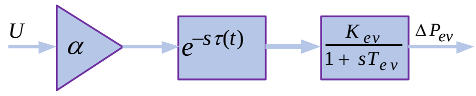


**Fig. 2. The EV aggregator with time-varying delay**

In some European countries like Germany, the Netherlands and Belgium, a PI controller was applied for frequency control [25]. Due to the PI controller's practical implementation in many different systems, this controller is selected for frequency control in the LFC scheme. The participation ratios $\alpha_1, \alpha_2, ....and\, \alpha_N$ represent each EV aggregator contribution in frequency control service and $\alpha_0$ indicates the generator participation factor. The PI controller output (control commands) is sent to the synchronous generator and N numbers of EV aggregators. In Fig. 1, $u(t)$ is the controller output, $R$ is the speed regulation factor, $\beta$ is the frequency bias factor. It should be noted that the summation of all the participation factors (generator and EVs) should equal 1.

### 2.1. Synchronous generator model

The synchronous generator can detect load variations instantly by using power control mechanisms [26]. When load demand fluctuates, the generator modifies its fuel consumption and its output electrical power. The synchronous generators are modeled via a first-order transfer function. The dynamic model of the synchronous generator used for frequency control studies was presented in Ref. [24]. It is to be noted that synchronous generators are equipped for the governor.

### 2.2. Presence of EV aggregators with the time-varying delay in LFC system

As explained, applying the EV battery in the LFC scheme causes a great improvement in system performance. The mathematical model of the EV battery that was presented as the first-order transfer function often as follows [27]:

$$H_{ev}(s)=\frac{K_{ev}}{1+sT_{ev}} \qquad (1)$$

Where, $K_{ev}$ and $T_{ev}$ are the gain and the battery time constant of EV, respectively. The term $e^{-s\tau(t)}$ is utilized to shape the delay in sending commands from the EV aggregator. The term $\tau(t)$ in this transfer function demonstrates the time-varying delay present while transferring the data from the open communication grid. Presuming that all EVs have a similar delay characteristic and time constant, an equivalent EV aggregator model with one delay function is obtained.

Fig. 2 shows the EVs aggregator model and its participation coefficient with time-varying delay. The single-area LFC system with $N$ numbers of EV aggregators could be calculated as follows:

$$\dot{x}(t)=\begin{bmatrix}\Delta\dot{f}\\ \Delta\dot{P}_m\\ \Delta\dot{P}_g\\ \Delta\dot{P}_{ev,1}\\ \vdots\\ \Delta\dot{P}_{ev,N}\end{bmatrix}=\begin{bmatrix}\frac{-D}{M} & 0 & \frac{1}{M} & \frac{1}{M} & \cdots & \frac{1}{M}\\ \frac{-1}{RT_g} & \frac{-1}{T_g} & 0 & 0 & \cdots & 0\\ 0 & \frac{1}{T_c} & \frac{-1}{T_c} & 0 & \cdots & 0\\ 0 & 0 & 0 & \frac{1}{T_{ev,1}} & \cdots & 0\\ \vdots & \vdots & \vdots & \ddots & \cdots & 0\\ 0 & 0 & 0 & 0 & \cdots & \frac{1}{T_{ev,N}}\end{bmatrix}\begin{bmatrix}\Delta f\\ \Delta P_m\\ \Delta P_g\\ \Delta P_{ev,1}\\ \vdots\\ \Delta P_{ev,N}\end{bmatrix}$$

$$+\begin{bmatrix}0\\ \frac{\alpha_0}{T_g}\\ 0\\ 0\\ \vdots\\ 0\end{bmatrix}u(t)+\sum_{j=1}^{N}\frac{\alpha_j K_{ev,j}}{T_{ev,j}}.u(t-\tau_k(t))+\begin{bmatrix}\frac{-1}{M}\\ 0\\ 0\\ 0\\ \vdots\\ 0\end{bmatrix}\Delta P_d \tag{2}$$

$$y=[\beta \quad 0 \quad 0 \quad 0 \quad \cdots \quad 0]\begin{bmatrix}\Delta f\\ \Delta P_m\\ \Delta P_g\\ \Delta P_{ev,1}\\ \vdots\\ \Delta P_{ev,N}\end{bmatrix}$$

$\Delta f, \Delta P_m, \Delta P_g$ and $\Delta P_{ev,i}$ are the variation of the frequency, mechanical and generator output power and $i$th EV aggregator electric power, respectively.

## 3. STABILITY ANALYSIS OF DELAYED SYSTEM

Suppose the delayed system stability depends on the delay size and information, in other words. In that case, the system stability region is determined by considering the time delay effects and the stability analysis known as delay-dependent stability. Lyapunov-Razumikhin theorem as a delay-dependent stability approach was used for robust stabilization of the delayed system [28]. It should be noted that this theorem for calculating the delay margin is conservative. Thus, the Lyapunov-Krasovskii theorem, which has less conservatism, is proposed. Actually, reducing the conservatism in the system stability analysis depends on selecting a suitable Lyapunov-Krasovskii functional approach and bounding inequality in the LMI framework.

### 3.1. Presented stability criteria considering a single time-varying delay

The single time-varying delay based linear system is considered as:

$$F_1=\dot{x}(t)=Ax(t)+A_d x(t-\tau(t)) \tag{3}$$

$$x(t)=\varphi(t)\ ,\ t\in[-\tau^M,0]$$

$$0\le\tau(t)\le\tau^M,\ \ \dot{\tau}(t)\le 1$$

Where, $x(t)$, $A$ and $A_d$ represent the system state vector, the state coefficient matrix and constant matrix. The initial condition $\phi(t)$ is a continuously differentiable function. $\tau(t)$ is a time-varying differentiable function and satisfies in Eq. (3). The term $\tau^M$ is used to show the upper bound of $\tau(t)$. Before applying the presented theorem, the PI controller is converted into the output feedback problem [29]. The closed-loop state space model is obtained from this transformation usage as:

$$X(t)=\begin{bmatrix}x^T & \int y^T\end{bmatrix}^T,\ \ Y(t)=\begin{bmatrix}y^T & \int y^T\end{bmatrix}^T \tag{4}$$

$$\begin{aligned}\dot{X}(t)&=A_0X(t)+A_dX\ (t-\tau(t)\ )\\ Y(t)&=CX(t)\end{aligned} \tag{5}$$

Where,

$$A_0=\begin{bmatrix}A & 0\\ c & 0\end{bmatrix},\ B=\begin{bmatrix}b+b_k\\ 0\end{bmatrix},\ C=\begin{bmatrix}c & 0\\ 0 & 1\end{bmatrix},\ A_d=-BKC$$

Where, $b$, $b_k$ and $c$ are the constant coefficients

***Theorem 1*** ([30]): The system $F_1$ is stable asymptotically for delay $\tau(t)$ if there are $P_1=P_1^T>0$, $S>0$, $P_i, i=2,3,4$, $Y_1,Y_2,Z_1,Z_2,Z_3$ and $R>0$ so that satisfy the following LMI:

$$\begin{bmatrix}L_1 & L_2 & L_3\\ * & L_4 & L_5\\ * & * & L_6\end{bmatrix}\le 0 \tag{6}$$

$$\begin{bmatrix}R & Y_1 & Y_2\\ * & Z_1 & Z_2\\ * & * & Z_3\end{bmatrix}\ge 0 \tag{7}$$

Where,

$$L_1=P_2^TA+A^TP_2+S+Y_1+Y_1^T+\tau^MZ_1$$

$$L_2=P_1-P_2^T+A^TP_3+Y_2+\tau^MZ_2;\ \ L_3=A^TP_4-Y_1^T+P_2A_d^T$$

$$L_4=-P_3-P_3^T+\tau^M(R+Z_3);\ \ L_5=-P_4-Y_2^T+P_3^TA_d$$

$$L_6=-(1-\mu)S+A_d^TP_4+P_4^TA_d$$

Proof. Please refer to [30].

### 3.2. Multiple time-varying delays based stability analysis

The multiple time-varying delays $\tau_1(t),\tau_2(t),...,\tau_n(t)$ based linear system is written as:

$$F_2 = \dot{x}(t) = Ax(t) + \sum_{i=1}^{n} A_{di} x(t - \tau_i(t))$$
$$x(t) = \varphi(t), t \in [-\tau^M, 0] \quad (8)$$

Now, stability criterion for linear systems with multiple time-varying delays is illustrated.

***Theorem 2:*** The system ( $F_2$ ) is asymptotically stable if there is exist real symmetric matrix $P > 0$ and real symmetric matrices $Q_{1i}, Q_{2i}, R_i > 0 \ (i = 1,2,..., N)$ and constant matrices $X$ with suitable dimensions $\psi_{i,l}^{(k)}$ so that the following LMI hold for $\tau_i \ \ (i = 1,2,..., N)$:

$$\hat{Z}_1 = \begin{bmatrix} Z_1 & X \\ * & Z_1 \end{bmatrix} \geq 0, \ \tilde{Z}_{i,l}^{(k)} = \begin{bmatrix} \tilde{Z}_i & \psi_{i,l}^{(k)} \\ * & \tilde{Z}_i \end{bmatrix} \geq 0 \quad (9)$$

$$\Xi(\tau_1,..., \tau_N) = 2Y_0^T P Y_2(\tau_1,..., \tau_N) + \theta - \frac{\Gamma^T \hat{Z}_1 \Gamma}{(\tau_1^M)^2} + Y_1^T (\sum_{i=1}^{N} Z_i) Y_1 - \sum_{i=2}^{N} \frac{(\Sigma_i^{(k)})^T \hat{Z}_i^{(k)} \Sigma_i^{(k)}}{(\tau_i^M)^2} \quad (10)$$

The rising order values of $0, \tau_{i-1}, \tau_{i-1}^M, \tau_i, \tau_i^M$ are defined as $\alpha_{i,0}, \cdots, \alpha_{i,4}$ for $2 < i < N$. Due to time dependency of $\hat{Z}_{i,l}^{(k)}$, $\Sigma_i^{(k)}$ and $Y_2(\tau_1, \ldots \tau_N)$, Eq. (10) could have several different forms. The different forms of $\Sigma_i^{(k)}$ are expressed in Fig. 3.

Notation: $W_i \in R^{n \times (6N-3)n}, i = 1, 2, \cdots, 6N-3$. The $W_i$ matrix has $(6N\text{-}3)n \times n$ blocks that i-th block is an identity matrix and other arrays are set to zeros. Also, proof of theorem 2 and all parameters of (10) are illustrated in Appendix A. After stability analysis, the LFC scheme containing EV aggregator with time-varying delay and obtaining the delay margin, the LFC scheme performance is evaluated in MATLAB/Simulink. A sinus wave function is considered to model time-varying delay in the MATLAB environment [22]. This sinus function amplitude and bias are equal to 2.

## 4. SIMULATION RESULTS

The effect of time-varying delays of EV aggregators on LFC system performance due to their fast response characteristic is important. Initially, stability analysis of the LFC system, including a single EV aggregator, is considered. The effects of multiple time-varying delay created by several EV aggregators participation in frequency control service are investigated. The parameters which have been used in simulations are given in Appendix B. The maximum allowable delay in the LFC scheme for the selected PI controller gains is calculated by the LMI lab. It should be noted that the LMI lab is a robust and efficient toolbox for finding out the LMI problem solution.

**Table 1. The maximum allowable delay for single EVs aggregator with $\alpha_1 = 0.2$**

| | Ki | | | | | | |
|---|---|---|---|---|---|---|---|
| Kp | 0.05 | 0.15 | 0.25 | 0.35 | 0.45 | 0.55 | 0.65 |
| 0.1 | ∞ | ∞ | 10.4043 | 6.3607 | 1.3192 | 0.94 | 0.5601 |
| 0.2 | ∞ | ∞ | 10.2661 | 6.2468 | 2.2261 | 0.7050 | 0.6710 |
| 0.3 | ∞ | 11.1804 | 9.1707 | 6.1597 | 2.1476 | 0.6348 | 1.1215 |
| 0.4 | 9.1118 | 8.1063 | 7.0998 | 6.0925 | 2.0848 | 0.5060 | 0.6701 |
| 0.5 | 7.0525 | 7.0484 | 6.0438 | 5.0386 | 2.0329 | 0.8068 | 0.8434 |
| 0.6 | 6.0042 | 6.0011 | 5.9976 | 4.9937 | 2.9895 | 1.0849 | 1.0801 |
| 0.7 | 5.9635 | 5.9611 | 4.9584 | 4.9554 | 2.9521 | 1.1486 | 1.2449 |
| 0.8 | 4.9284 | 4.9265 | 4.9234 | 3.9220 | 2.9194 | 1.1367 | 1.4138 |
| 0.9 | 4.8976 | 3.8960 | 3.8943 | 3.8925 | 2.8904 | 1.1883 | 1.4895 |
| 1 | 3.8701 | 3.8689 | 3.8675 | 3.8660 | 2.8644 | 1.2027 | 1.4908 |

**Table 2. The maximum allowable delay for single EVs aggregator with $\alpha_1 = 0.4$**

| | $K_i$ | | | | | | |
|---|---|---|---|---|---|---|---|
| $K_p$ | 0.05 | 0.15 | 0.25 | 0.35 | 0.45 | 0.55 | 0.65 |
| 0.1 | 20.2635 | 6.8210 | 4.4043 | 2.3607 | 1.3192 | 1.2501 | 0.2601 |
| 0.2 | 8.7510 | 5.7400 | 4.2661 | 2.2468 | 1.2261 | 1.2050 | 0.3710 |
| 0.3 | 5.4892 | 4.1804 | 3.1707 | 2.1597 | 1.1476 | 1.1348 | 0.4215 |
| 0.4 | 3.1118 | 3.1063 | 3.0998 | 2.0925 | 1.0848 | 1.7060 | 0.5701 |
| 0.5 | 3.0525 | 3.0484 | 3.0438 | 2.0386 | 1.0329 | 1.8068 | 0.6434 |
| 0.6 | 2.0042 | 2.0011 | 2.9976 | 1.9937 | 1.9895 | 1.9849 | 0.6801 |
| 0.7 | 2.9635 | 2.9611 | 2.9584 | 1.9554 | 1.9521 | 1.9486 | 0.7449 |
| 0.8 | 1.9284 | 1.9265 | 1.9244 | 1.9220 | 1.9194 | 1.9167 | 0.7638 |
| 0.9 | 1.8976 | 1.8960 | 1.8943 | 1.8925 | 1.8904 | 1.9883 | 0.8895 |
| 1 | 1.8701 | 1.8689 | 1.8675 | 1.8660 | 1.8644 | 2.0627 | 0.8908 |

### 4.1. Case 1: LFC including single EVs aggregator

The frequency oscillations under different PI controller gains are presented in Fig. 4. As shown, when (Ki , Kp) are set to (0.5, 0.5), the capability of the LFC system for damping the oscillation is reduced and consequently, the LFC system becomes unstable. LFC system's stability depends on the correct selection of PI controller parameters. By increasing the $K_p$ at constant $K_i$ gain, the settling time is diminished. Since $K_i$ value becomes larger, the rising time is improved while settling time is degraded. The optimal design of the PI controller in the stability region leads to improve the LFC scheme performance. The maximum allowable delay $\tau^M$ of the single EVs aggregator is computed at two participation ratios of 0.2 and 0.4. The obtained values are listed in Tables 1 and 2, respectively. By rising the $K_i$ gain, $\tau^M$ reduces. In fact, the LFC system's sensitivity to the EV aggregator's time-varying delay is more than the previous value of $K_i$. Deviations of $K_p$ has variable effects on the maximum allowable delay that depends on the $K_i$ value. If the $K_i$ gain is selected in the interval of [0.2, 0.6], due to $K_p$ rising, $\tau^M$ decreases. But, if the value of $K_i$ is equal to 0.65, $\tau^M$ will be increased by growing the $K_p$ value. When the value of $K_i$ is fixed at..0.55, first $\tau^M$ decreases and then as $K_p$ value increases, $\tau^M$ increases again. The maximum allowable delay reduces because of participation ratio $\alpha_1$ has increased. The allowable upper bound of delay calculated is greater for low values of $K_p$ and $K_i$. In other words, the LFC scheme has more robust to time-varying delay. As known, selecting the PI controller with these small gains can result in a weak performance of the LFC system. For $K_p$ gains larger than 0.5, the maximum allowable delay has a low variation by increments of $K_i$. When the participation ratio of the EVs aggregator is higher, it means that the contribution of EVs aggregator in frequency control has increased. In this case, since the LFC system performance is affected by EVs aggregator widely, the presence of EVs aggregator is very important.

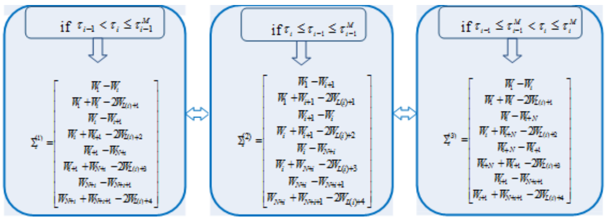

Fig. 3. The different forms of $\Sigma_i^{(k)}$

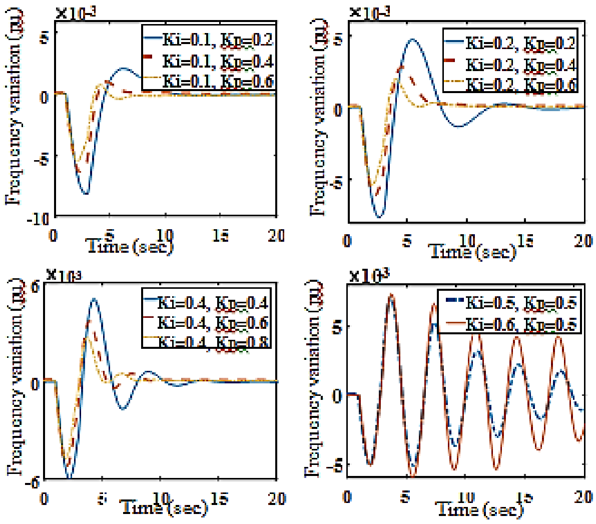


Fig. 4. Frequency variations for different values of (Ki , Kp)

Therefore, the upper bound of delay $\tau^M$ is decreased. The LFC system root locus with a single EV aggregator, the effect of adding the time-varying delay and PI controller are illustrated in Figs. 5 to 7. According to Figs. 5 to 7, considering the time-varying delay in the state-space model of the LFC system leads to create the one right and three left zeros. Also, delay existence adds four stable poles to the root locus of the LFC system. It is noted that the time-varying delay model is estimated by three-order estimation. For positive gain margin, the LFC system becomes unstable and the magnitude of frequency oscillation gets large. Adding the PI controller to the network increases the gain margin and enhances the LFC scheme performance. The gain margin with the PI controller is 26.7. Fig. 8 shows the stability region of the LFC system for PI controller parameters. To design the PI controller and draw the graph between $K_i$ and $K_p$ for $K_d = 0$, the presented calculations in Ref. [31] are used.

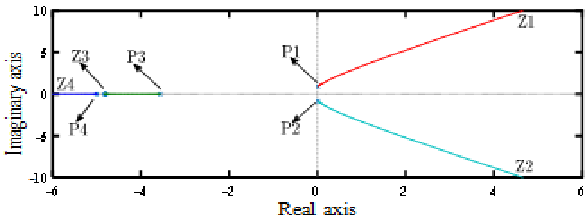


Fig. 5. Root locus of LFC system with single EVs aggregator

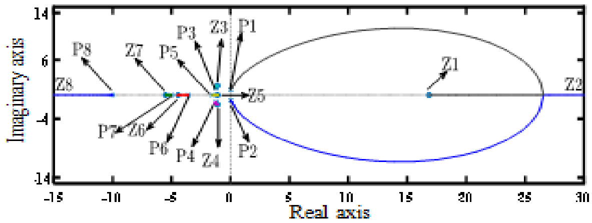


Fig. 6. Root locus of LFC system including single EVs aggregator with time-varying delay

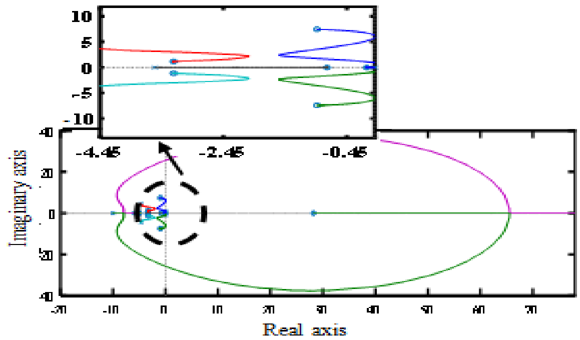


Fig. 7. Root locus of LFC system including single EVs aggregator with time-varying delay and PI controller

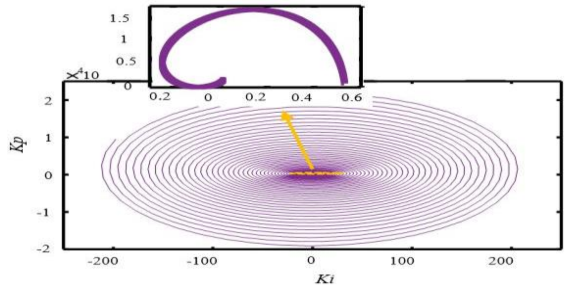


**Fig. 8. Stability region of PI controller for a random value of $\tau$ in [0,4]**

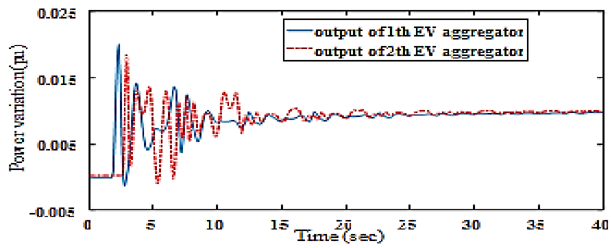


**Fig. 9. Power variations of two EV aggregators with the same participation ratio for $\Delta P_d = 0.05$**

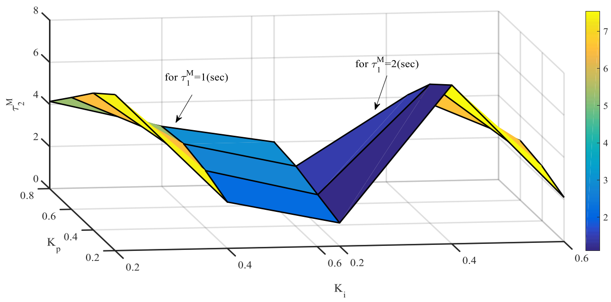


**Fig. 10. Maximum allowable delay of EV aggregator 2 when $\alpha_1 + \alpha_2 = 0.2$ and $\alpha_2 = 9\alpha_1$**

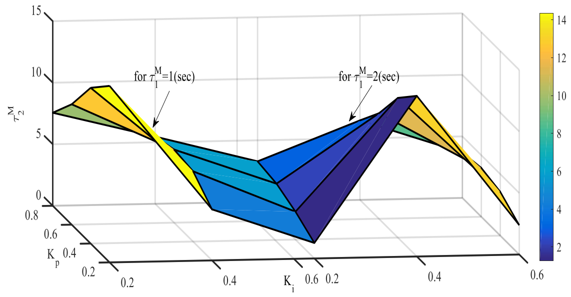


**Fig.11. Maximum allowable delay of EV aggregator 2 when $\alpha_1 + \alpha_2 = 0.2$ and $\alpha_2 = \alpha_1$**

### 4.2. Case 2: LFC including two EV aggregators with time-varying delay

The maximum allowable delays ($\tau_1^M, \tau_2^M$) of two EV aggregators for different PI controller parameters and dissimilar combinations of $\alpha_1$ and $\alpha_2$ are investigated. In this work, one the maximum allowable delay $\tau_2^M$ is obtained when $\tau_1^M$ is set to constant values of 0.001, 0.1, 1, 2 and 5 seconds The obtained results are listed in Tables 3 and 4. As seen, the maximum allowable delay $\tau_2^M$ becomes lower when $K_i$ gain increases. This conclusion is obtained for a single EVs aggregator, also. The $K_p$ variation has a different effect on the maximum allowable delay such that according to $K_i$ changing, the $\tau_2^M$ experiences different orientations. The obtained result is described as follows:

$$\text{If}\{K_i = 0.2, K_p \uparrow \Rightarrow \tau_2^M \downarrow\}$$

$$\text{If}\{K_i = 0.4, K_p \uparrow \Rightarrow \text{At first, } \tau_2^M \uparrow \text{ and then} \downarrow\}$$

$$\text{If}\{K_i = 0.6, 0.2 \le K_p \le 0.8 \text{ and } K_p \uparrow \Rightarrow \tau_2^M \uparrow\}$$

$$\text{If}\{K_i = 0.6, K_p > 0.8 \text{ and } K_p \uparrow \Rightarrow \tau_2^M \downarrow\}$$

**Table 3. The greatest allowable delay $\tau_2^M$ when $\alpha_1 = \alpha_2 = 0.2,\ \alpha_1 + \alpha_2 = 0.4$**

| | | $K_i = 0.2$ | | | | $K_i = 0.4$ | | | | $K_i = 0.6$ | | | |
|---|---|---|---|---|---|---|---|---|---|---|---|---|---|
| $\tau_1^M$ | Kp | 0.2 | 0.4 | 0.6 | 0.8 | 0.2 | 0.4 | 0.6 | 0.8 | 0.2 | 0.4 | 0.6 | 0.8 |
| | 0.001 | 8.57 | 8.18 | 6.56 | 5 | 3.75 | 4.75 | 4.89 | 4.31 | 2.1 | 2.5 | 3.12 | 3.34 |
| | 0.1 | 7.84 | 7.35 | 6.26 | 4.57 | 3.06 | 4.5 | 4.68 | 3.99 | 1.79 | 2.24 | 2.9 | 2.76 |
| | 1 | 5.66 | 5.28 | 4.00 | 2.7 | 1.57 | 2.3 | 2.38 | 2.00 | * | 1 | 1.36 | 1.23 |
| | 2 | 4.12 | 3.86 | 2.07 | * | * | * | * | * | * | * | * | * |
| | 5 | * | * | * | * | * | * | * | * | * | * | * | * |

**Table 4. The greatest allowable delay $\tau_2^M$ when $\alpha_2 = 9\alpha_1,\ \alpha_1 + \alpha_2 = 0.4$**

| | | $K_i = 0.2$ | | | | $K_i = 0.4$ | | | | $K_i = 0.2$ | | | |
|---|---|---|---|---|---|---|---|---|---|---|---|---|---|
| $\tau_1^M$ | Kp | 0.2 | 0.4 | 0.6 | 0.8 | 0.2 | 0.4 | 0.6 | 0.8 | 0.2 | 0.4 | 0.6 | 0.8 |
| | 0.001 | 3.35 | 3.09 | 2.56 | 2.1 | 1.54 | 1.75 | 1.79 | 1.43 | 0.98 | 1.20 | 1.39 | 1.2 |
| | 0.1 | 3.31 | 3.02 | 2.51 | 1.96 | 1.51 | 1.64 | 1.62 | 1.36 | 0.87 | 1.24 | 1.37 | 1.14 |
| | 1 | 3.11 | 2.88 | 2.45 | 1.67 | 1.28 | 1.52 | 1.48 | 1.31 | * | 1.1 | 1.19 | 1.12 |
| | 2 | 3.00 | 2.67 | 2.27 | * | * | * | * | * | * | * | * | * |
| | 5 | * | * | * | * | * | * | * | * | * | * | * | * |

Although the allowable delay has a minimum value for $(K_p, K_i) = (0.2, 0.6)$, the LFC scheme is unstable at low proportional and high integral gains. By increasing the $K_p$ parameter, the PI controller becomes stable. To provide the LFC model's desired performance, including two EV aggregators, if the maximum allowable delay of each EV aggregator increases, the other should be reduced. As shown, when $\tau_1^M$ increases, $\tau_2^M$ reduces. When the sum of the EV aggregators participation ratio increases, their maximum allowable delay decreases. The delay of aggregators with a large participation ratio has more effects on frequency control services. In other words, the participation ratio of each aggregator is considered to determine their maximum allowable delay. By decreasing the sum of the contribution ratio of aggregators, $\tau_2^M$ has reduced. If two EV aggregators have the same time-varying delay characteristics and the sum of their contribution is equal to the contribution of the single EVs aggregator, considerable results are obtained by comparing single and two aggregators. For example, the greatest allowable delay of a single EV aggregator is computed as 4.9234 for $\alpha_1$, $K_i$ and $K_p$ equal to 0.2, 0.2, 0.8, respectively. According to the maximum allowable delay for a single EV aggregator, the LFC scheme containing two EV aggregators is unstable for $\alpha_1+\alpha_2=0.2$, $K_i=0.2$ and $K_p=0.8$ at $\tau_1{}^M=5$. The maximum allowable delays of EV aggregator 2 for different participation ratios are shown in Figs. 10 and 11. According to Figs. 10 and 11, the maximum allowable delay $\tau_2{}^M$ increases when the sum of the contribution of EV aggregators decreases. In other words, when the contribution of each EV aggregator in frequency control service rises, its maximum allowable delay decrease.

## 5. CONCLUSION

Many electric vehicle applications and their increasing participation in frequency regulation markets lead to enhanced LFC models' efficiency. The presence of the EV aggregators in the LFC system leads to time-varying delays. The stability analysis of the LFC system with single and multiple time-varying delays is presented in this paper. The remarkable achievements of this paper are as follows.

- Presenting the candidate Lyapunov-Krasovskii function and LMI equation for obtaining a maximum allowable delay of EV aggregators.
- Investigating the participation ratio and PI parameters variation on the maximum allowable delay value.
- Obtaining the stability region of the LFC with single EV aggregators and its variation for two EV aggregators.
- Drawing the LFC system root locus with and without time-varying delay.
- Reducing the conservatism in the evaluation of the maximum allowable delay and present a larger maximum allowable delay in the presence of the electric vehicles.
- Using a small dimension of LMI equations for the delay-based stability of load frequency controller system.

The presented stability analysis could help to obtain the EV aggregators delay in the frequency control for a considered PI controller.

Appendix A

The selected Lyapunov-Krasovskii function of LFC system, including multiple time-varying delays are presented as:

$$V(x_t)=\xi^T(t)P\xi(t)+\sum_{i=1}^{N}\int_{t-\tau_i^M}^{t}x^T(s)Q_{1,i}x(s)\,ds+ \sum_{i=1}^{N}\int_{t-\tau_i}^{t}x^T(s)Q_{2,i}x(s)\,ds+\sum_{i=1}^{N}\frac{1}{\tau_i^M}\int_{-\tau_i^M}^{0}\int_{t+\theta}^{t}\dot{x}^T(s)R_i\,\dot{x}(s)\,ds\,d\theta \tag{A.1}$$

The time-derivative of Eq. (A.1) is found to be:

$$\dot{V}(x_t)\le 2\xi^T(t)P\dot{\xi}(t)+\sum_{i=1}^{N}x^T(t)\,(Q_{1,i}+Q_{2,i})\,x(t) -\sum_{i=1}^{N}x^T(t-\tau_i^M)\,Q_{1,i}\,x(t-\tau_i^M)\text{-}\sum_{i=1}^{N}(1-\mu_i)\,x^T(t-\tau_i)\,Q_{2,i}\,x(t-\tau_i) +\sum_{i=1}^{N}(\tau_i^M)^2\dot{x}^T(t)\,R_i\,\dot{x}(t)\text{-}\sum_{i=1}^{N}\frac{1}{\tau_i^M}\int_{t-\tau_i^M}^{t}\dot{x}^T(t)\,R_i\,\dot{x}(t)\,ds \tag{A.2}$$

Now, an augmented vector $\chi(t)$ is introduced as:

$$\chi(t)=col\{x(t),x(t-\tau_1),\dots x(t-\tau_N),x(t-\tau_1{}^M) ,\dots,x(t-\tau_N^M),\frac{\int_{t-a_{2,1}}^{t-a_{2,0}}x(s)ds}{a_{2,1}},\dots\frac{\int_{t-a_{2,4}}^{t-a_{2,3}}x(s)ds}{a_{2,4}-a_{2,3}}, \dots,\frac{\int_{t-a_{N,4}}^{t-a_{N,3}}x(s)ds}{a_{N,4}-a_{N,3}}\} \tag{A.3}$$

Using of the $\chi(t)$, $\dot{\xi}(t)$ in Eq. (A.1) can be calculated as:

$$\dot{\xi}(t)=col\{A_0x(t)+\sum_{i=1}^{N}A_ix(t-\tau_i),x(t)-x(t-\tau_1^M),\dots,x(t)-x(t-\tau_N^M)\} =col\{\sum_{i=0}^{N}A_iE_{i+1},E_1-E_{1+N+1},\dots,E_1-E_{1+N+N}\}\chi(t)=G_0\chi(t)$$

(A.4)

By considering the $\chi(t)$, the $\xi(t)$ can be written as:

$$\xi(t)=col\{x(t),\int_{t-\tau_1^M}^{t}x(s)\,ds,\dots,\int_{t-\tau_N^M}^{t}x(s)\,ds\}= col\{E_1,G_{2,1},\frac{1}{2}(G_{2,2}+\sum_{k=1}^{4}(a_{2,k}-a_{2,k-1})E_{L(2)+k}\,, \dots,\frac{1}{2}(G_{2,N-1}+\sum_{k=1}^{4}(a_{N-1,k}-a_{N-1,k-1})\times E_{L(N-1)+k}\,), \sum_{k=1}^{4}(a_{N,k}-a_{N,k-1})E_{L(N)+k}\}\chi(t)=G_2(\tau_1,\dots,\tau_N)\chi(t) \tag{A.5}$$

According to the definition of matrices $\xi(t)$, $\dot{V}(x_t)$ could be rewritten as follows:

$$\dot{V}(x_t)\le\chi^T(t)\{2G_0{}^TPG_{2(\tau_1,\dots,\tau_N)}+\theta+ G_1^T(\sum_{i=1}^{N}(\tau_i^M)^2R_i)G_1\}\chi(t)\text{-}\sum_{i=1}^{N}\frac{1}{\tau_i^M}\int_{t-\tau_i^M}^{t}\dot{x}^T(s)R_i\dot{x}(s)ds \tag{A.6}$$

Wirtinger improved inequality usage for the last term of (A.2) leads to simplification of LKF time-derivative relation [32].

$$\frac{-1}{\tau_1^M}\int_{t-\tau_1^M}^{t}\dot{x}^T(s)R_i\dot{x}(s)ds=\frac{1}{\tau_1^M}(\int_{t-\tau_1}^{t}\dot{x}^T(s)R_i\dot{x}(s)ds)$$

$$+\int_{t-\tau_1^M}^{t-\tau_1}\dot{x}^T(s)R_i\dot{x}(s)ds\le\frac{1}{(\tau_1^M)^2}\chi^T(t)\Gamma^T\begin{bmatrix}\frac{\tau_1^M}{\tau_1}R_1 & 0\\ 0 & \frac{\tau_1^M}{\tau_1^M-\tau_1}R_1\end{bmatrix}\Gamma\chi(t)$$

(A.7)

From Lemma 1 (theorem 1 in Ref. [33]), when $K=2$ and $i=1$ if there exists a matrix X such that

$$\hat{R}_1=\begin{bmatrix}R_1 & X\\ 0 & R_1\end{bmatrix}\ge 0 \quad (A.8)$$

The following inequality is achieved:

$$\frac{-1}{\tau_1^M}\int_{t-\tau_1^M}^{t}\dot{x}^T(s)R_1\dot{x}(s)ds\le-\frac{1}{(\tau_1^M)^2}\chi^T(t)\Gamma^T\hat{R}_1\Gamma\chi(t) \quad (A.9)$$

The presented method is applied to Eq. (A.2) for $(2<i<N)$ By keeping the problem generality, *i* th and *(i-1)* th time-varying delays are considered as:

$$\frac{-1}{\tau_i^M}\int_{t-\tau_i^M}^{t}\dot{x}^T(s)R_i\dot{x}(s)ds=\frac{-1}{\tau_i^M}(\int_{t-\tau_{i-1}}^{t}\dot{x}^T(s)R_i\dot{x}(s)ds+ \quad (A.10)$$

$$\int_{t-\tau_i}^{t-\tau_{i-1}}\dot{x}^T(s)R_i\dot{x}(s)ds+\int_{t-\tau^M_{i-1}}^{t-\tau_i}\dot{x}^T(s)R_i\dot{x}(s)ds+\int_{t-\tau^M_i}^{t-\tau_{i-1}^M}\dot{x}^T(s)R_i\dot{x}(s)ds$$

We apply Lemma 2 in Ref. [32] to each integral as follows:

$$\frac{-1}{\tau_i^M}\int_{t-\tau_i^M}^{t}\dot{x}^T(s)R_i\dot{x}(s)ds\le-\chi^T(t)(\Sigma_i^{(1)})^TR_i^{(1)}\Sigma_i^{(1)}\chi(t) \quad (A.11)$$

$$R_i^{(1)}=diag(\frac{\tilde{R}_i\tau_i^M}{\tau_{i-1}},\frac{\tilde{R}_i\tau_i^M}{\tau_i-\tau_{i-1}},\frac{\tilde{R}_i\tau_i^M}{\tau_{i-1}^M-\tau_i},\frac{\tilde{R}_i\tau_i^M}{\tau_i^M-\tau_{i-1}^M})$$

According Lemma 1 when K=4, if there exists matrices $\psi_{i,l}^{(1)}, l=1,2,\ldots,6$. So, we have:

$$\hat{R}_{i,l}^{(1)}=\begin{bmatrix}\tilde{R}_i & \psi_{i,l}^{(1)}\\ * & \tilde{R}_i\end{bmatrix}\ge 0 \quad (l=1,\ldots,6) \quad (A.12)$$

The integral inequality is estimated as follows:

$$\frac{-1}{\tau_i^M}\int_{t-\tau_i^M}^{t}\dot{x}^T(s)R_i\dot{x}(s)ds\le\frac{-1}{(\tau_i^M)^2}\chi^T(t)(\Sigma_i^{(1)})^T\hat{R}_i^{(1)}\Sigma_i^{(1)}\chi(t) \quad (A.13)$$

$$\theta=diag\{\sum_{i=1}^{N}Q_{1i}+Q_{2i}-(1-\mu_1)Q_{21},\ldots,$$
$$-(1-\mu_N)Q_{2N},-Q_{11},\ldots,-Q_{1N},0_{4(N-1)}\} \quad (A.14)$$

$$Y_0=col\{\sum_{i=0}^{N}A_iW_{i+1},W_1-W_{N+1+1},\ldots,W_1-W_{N+1+N}\} \quad (A.15)$$

$$Y_1=\sum_{i=0}^{N}A_iW_{i+1},\ \Gamma=col\{W_1-W_2,W_2-W_{N+1+1}\} \quad (A.16)$$

$$Y_{2,i}=\begin{cases}\sum_{k=1}^{2}(a_{(i+1),k}-a_{(i+1),(k-1)})W_{L(i+1)+k} & \tau_i^M<\tau_{i+1}\\ \sum_{k=1}^{3}(a_{(i+1),k}-a_{(i+1),(k-1)})W_{L(i+1)+k} & \text{o.w}\end{cases} \quad (A.17)$$

$$Y_2=col\ \{W_1,Y_{2,1},\frac{1}{2}(Y_{2,2}+\sum_{k=1}^{4}a_{2,k}-a_{2,(k-1)})W_{L(2)+k}),$$
$$\ldots,\frac{1}{2}(Y_{2,(N-1)}+\sum_{k=1}^{4}a_{(N-1),k}-a_{(N-1),(k-1)})W_{L(N-1)+k}),$$
$$\sum_{k=1}^{4}(a_{N,k}-a_{N,(k-1)})\ W_{L(N-1)+k})\} \quad (A.18)$$

## Appendix B

| | |
|---|---|
| Inertia constant | $M=8.8$ |
| Load-damping factor | $D=1$ |
| Governor time constant | $T_g=0.2$ |
| Turbine time constant | $T_c=0.3$ |
| Fraction of total turbine power | $F_p=1.6$ |
| Battery gain | $K_{ev}=1$ |
| Battery time constant | $T_{ev}=0.1$ |
| Speed regulation | $R=1.11$ |
| Frequency bias factor | $\beta=40$ |
| Reheat time constant | $T_r=12$ |

## REFERENCES


[1] Y. Zheng et al., “Integrating plug-in electric vehicles into power grids: A comprehensive review on power interaction mode, scheduling methodology and mathematical foundation”, *Renew. Sustain. Energy Rev.*, vol. 112, pp. 424-439, 2019.

[2] A. Safari, F. Babaei, M. Farrokhifar, “A load frequency control using a PSO-based ANN for micro-grids in the presence of electric vehicles”, *Int. J. Ambient Energy.*, Vol. 42, pp. 688-700, 2021.

[3] D. Aravindh et al., “Design of observer-based non-fragile load frequency control for power systems with electric vehicles”, *ISA Trans*, vol. 91, pp. 21-31, 2019.

[4] K. Tan, V. Ramachandaramurthy, J. Yong, “Integration of electric vehicles in smart grid: A review on vehicle to grid technologies and optimization techniques”, *Renew. Sustain. Energy Rev.*, vol. 53, pp. 720-732, 2016.

[5] H. Liu et al., “Decentralized vehicle-to-grid control for primary frequency regulation considering charging demands”, *IEEE Trans. Power Syst.*, vol. 28, pp. 3480-89, 2013.

[6] J. Pillai, B. Bak-Jensen, “Integration of vehicle-to-grid in the western Danish power system”, *IEEE Trans. Sustain. Energy.*, vol. 2, pp. 12-19, 2010.

[7] M. Galus, S. Koch, G. Andersson, “Provision of load frequency control by PHEVs, controllable loads, and a cogeneration unit”, *IEEE Trans. Ind. Electron.*, vol. 58, pp. 4568-82, 2010.

[8] M. Sarker, Y. Dvorkin, M. Ortega-Vazquez, “Optimal participation of an electric vehicle aggregator in day-ahead energy and reserve markets”, *IEEE Trans. Power Syst.*, vol. 31, pp. 3506-15, 2015.

[9] M. Vayá, G. Andersson, “Optimal bidding strategy of a plug-in electric vehicle aggregator in day-ahead

electricity markets under uncertainty", *IEEE Trans. Power Syst*., vol. 30, pp. 2375-85, 2014.

[10] K. Ko, S. Han, D. Sung, "A new mileage payment for EV aggregators with varying delays in frequency regulation service", *IEEE Trans. Smart Grid*., vol. 9, pp. 2616-24, 2016.

[11] A. Molisch, "Wireless communications", John Wiley & Sons, 2012.

[12] C. Zhang et al., "Delay-dependent robust load frequency control for time delay power systems", *IEEE Trans. Power Syst*., vol. 28, pp. 2192-2201, 2013.

[13] Ş. Sönmez, S. Ayasun, C. Nwankpa, "An exact method for computing delay margin for stability of load frequency control systems with constant communication delays", *IEEE Trans. Power Syst*., vol. 31, pp. 370-7, 2015.

[14] R. Zhang et al., "New approaches to stability analysis for time-varying delay systems", *J. Franklin Inst*., vol. 356, pp. 4174-89, 2019.

[15] C. Duan et al., "Structure-exploiting delay-dependent stability analysis applied to power system load frequency control", *IEEE Trans. Power Syst.,* vol. 32, pp. 4528-40, 2017.

[16] K. Ramakrishnan, G. Ray, "Stability criteria for nonlinearly perturbed load frequency systems with time-delay", *IEEE J. Emerging Sel. Top. Circuits Syst*., vol. 5, pp. 383-92, 2015.

[17] A. Khalil et al., "The impact of the time delay on the load frequency control system in microgrid with plug-in-electric vehicles", *Sustain. Cities Soc.*., vol. 35, pp. 365-77, 2017.

[18] S. Sönmez, S. Ayasun, "Stability region in the parameter space of PI controller for a single-area load frequency control system with time delay", *IEEE Trans. Power Syst*., vol. 31, pp. 829-30, 2015.

[19] C. Zhang et al., "Further results on delay-dependent stability of multi-area load frequency control", *IEEE Trans. Power Syst*., vol. 28, pp. 4465-74, 2013.

[20] V. Çelik, M. Özdemir, G. Bayrak, "The effects on stability region of the fractional-order PI controller for one-area time-delayed load–frequency control systems", *Trans. Inst. Meas. Control.*, vol. 39, pp. 1509-21, 2017.

[21] P. Ojaghi, M. Rahmani, "LMI-based robust predictive load frequency control for power systems with communication delays", *IEEE Trans. Power Syst*., vol. 32, pp. 4091-100. 2017.

[22] F. Yang et al., "Auxiliary-function-based double integral inequality approach to stability analysis of load frequency control systems with interval time-varying delay", *IET Control Theory Appl*., Vol. 12, pp. 601-12, 2017.

[23] L. Jin et al., "Delay-dependent stability analysis of multi-area load frequency control with enhanced accuracy and computation efficiency", IEEE Trans. Power Syst., vol. 34, pp. 3687-96 2019.

[24] K. Ko, D. Sung, "The effect of EV aggregators with time-varying delays on the stability of a load frequency control system", *IEEE Trans. Power Syst*., vol. 33, pp. 669-80, 2017.

[25] Y. Rebours et al., "A survey of frequency and voltage control ancillary services-Part I: Technical features", *IEEE Trans. Power Syst.*, vol. 22, pp. 350-57, 2007.

[26] M. Khooban, T. Niknam, "A new intelligent online fuzzy tuning approach for multi-area load frequency control: self adaptive modified bat algorithm", *Int. J. Electr. Power Energy Syst*., vol. 71, pp. 254-261, 2015.

[27] F. Babaei et al., "SSA based Fractional-Order PID Controller for LFC Systems in the Presence of Delayed EV aggregators", *IET Electr. Syst*., vol. 10, pp. 259-67, 2020.

[28] R. Dey, G. Ray, V. Balas, "Stability and stabilization of linear and fuzzy time-delay systems: a linear matrix inequality approach", Springer, 2017.

[29] F. Zheng, Q. Wang, T. Lee, "On the design of multivariable PID controllers via LMI approach", *Automatica*., Vol. 38, pp. 517-26, 2002.

[30] V. Suplin, E. Fridman, U. Shaked, "H/sub/splinfin/control of linear uncertain time-delay systems-a projection approach", *IEEE Trans. Autom. Control.*, vol. 51, pp. 680-85, 2006.

[31] N. Chowdary, M. Chidambaram, "Robust controller design for first order plus time delay systems using kharitonov theorem", *IFAC Proc. Vol.,* vol. 47, pp. 184-91, 2014.

[32] A. Seuret, F. Gouaisbaut, "Wirtinger-based integral inequality: application to time-delay systems", *Automatica,* vol. 49, pp. 2860-66, 2009.

[33] P. Park, J. Ko, C. Jeong, "Reciprocally convex approach to stability of systems with time-varying delays", *Automatica*., vol. 47, pp. 235-38, 2011.